International Journal of Innovative Technologies
WWW.IJITECH.ORG
ISSN 2321-8665
Vol.05,Issue.01,
January-2017,
Pages:0051-0055

Performance of Grid Connected Improved Active Power Filter With SMES Module

M. SOUMYA[1], B. RATNAJI[2]

[1]PG Scholar, Vignana Bharathi Institute of Technology, Hyderabad, India, E-mail: muskesam@gmail.com.
[2]Assistant Professor, Vignana Bharathi Institute of Technology, Hyderabad, India, E-mail: bratnaji33@gmail.com.

Abstract: In distribution generation many types of loads are connected, linear non linear balanced and unbalanced loads. Theses loads consume a large reactive power from the conventional grid source, reducing the power quality and increase of harmonics in the distribution grid. These power quality issues are to be minimized with active power filters, by injecting reactive power into the distribution system. The distribution system is a four wire connected source and load, making the active power filter also to be a four legged inverter. The active power filter has a DC link capacitor at the DC side and harmonic filters in the AC side. The DC side of the converter is connected to a SMES module, which stores the energy from the converter. To achieve digitalized control of the power electronic switches in the active power filter space vector PWM is used. Modeling and analysis of the modules are designed in MATLAB Simulink software with reports of graphs and parametric values.

Keywords: SMES (Super Conducting Energy Storage), MATLAB, Simulink.

I. INTRODUCTION

Distribution generation has been the replacement for the traditional generation of power using fossil fuels. Renewable energy sources can be used for the generation of power by the usage of Sun irradiation, wind or bio mass. These production of power reduces the pollution caused by the other ways of generation and can be notified as eco-friendly sources. In this paper we consider PVA (Photo Voltaic Array) sources [1] which generate power with the use of solar irradiation. The main aim of this paper is to inter-connect this PVA to the grid with the help of filters and inject required reactive power to the loads so as to compensate the load reactive power demand. This facility of the PVA reduces the consumption of reactive power from the main source improvising the system quality. As the reactive power reduces the power factor improves, which in turn reduces the total harmonic distortion. The integration of these renewable resources utilizing Sun and wind sources in the distribution system can be defined as distribution generation systems. The penetration [2] of these resources is limited by the supply of percentage to load demanded. The system is said to be 100% penetrated when the total load is supplied by the renewable sources as shown in Fig.1. Due to the integration of these renewable sources into the grid with power electronic devices may deteriorate the power quality. We need to compensate the quality with FACTs devices in a combination of passive filters.

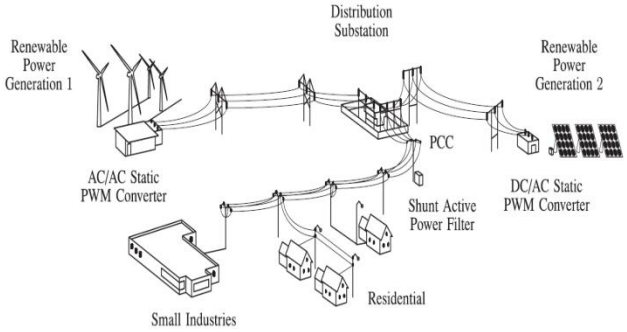

Fig. 1.Distribution grid with RES.

In order to interconnect the renewable sources (PVA) to the grid system a conversion is required to convert the DC to three phase AC. The three phase AC [3] has to be in synchronization with the grid in parameters of voltage, frequency and phase. The VSI (Voltage source Inverter) is a four legged eight IGBT switch inverter, where the DC side is connected to capacitor and the three phase AC side connected to the grid through LC filter. The LC filter is connected to damp out the generated harmonics form the VSI [3] avoiding the harmonics into the grid as shown in Fig.2.

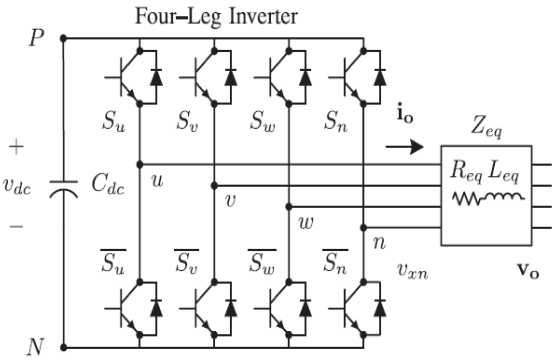

Fig. 2. VSI connected to grid using DC capacitor.

Any disruption in the switching of the VSI while connected to the grid system may also disrupt the grid voltage increasing the vulnerability of equipment connected to the system. It is very mandatory to maintain the switching of the VSI with

optimal control techniques. Adding to the above load issues we also have sag and swell [4] of voltage problems where swell is considered most critical problem in the entire electrical engineering. Sags may not cause immediate damage to the system but it causes insipient damage to the equipment. Swells are caused when large loads in the range of mega watts are suddenly disconnected from the distribution system. It can be elaborated as when the distribution system is feeding large loads high currents flow in the lines, but when this large load is disconnected the consumption current is reduced immediately in the line. In order to maintain the apparent power in the distribution line the voltage increases suddenly creating a voltage swell in the system. This effect is called Ferranti effect. The increased voltage may be 125-150% [5] to the nominal voltage value which can be eliminated with either circuit breakers or FACTs devices such as DVR or UPQC.

On the other hand the sags are created when a large load is suddenly connected to the distribution system. Due to the sudden adding of large load the current in the line is increased suddenly and as we discussed above to maintain the apparent power the voltage now will be decreased and sag is created. The system is said to be in sag when the voltage level goes below 95% of the nominal value as shown in Fig.3.

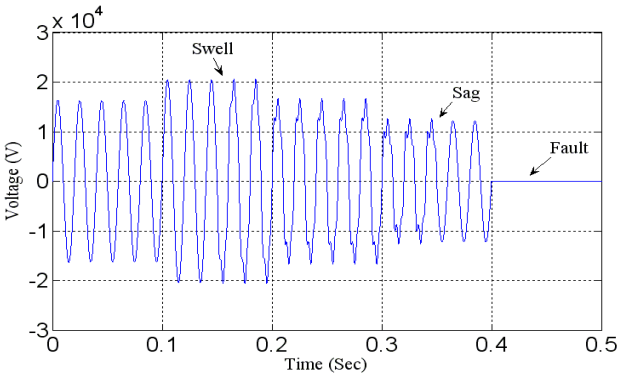

Fig. 3. Voltage profile with sag, swell & harmonics.

II. CONTROL OF FOUR LEGGED CONVERTER

A dq component [6] current reference generator method is utilized to get the active power filter topology current reference signals. This proposed idea presents a quick and precise signal tracking ability. This feature avoids voltage disruptions that get worse when the current reference signal disturbing compensation routine. The current orientation signals are obtained from the equivalent to load currents as shown in Fig. 4. This element calculates the reference signal currents necessary by the converter to give back reactive power, current harmonic, and current inequity. The dislocation power factor (sin φ(L)) [7] and the utmost total harmonic distortion of the load (THD(L)) defines the associations between the obvious power necessary by the active power filter, with reverence to the load, as shown

$$\frac{S_{\mathrm{APF}}}{S_L} = \frac{\sqrt{\sin\phi_{(L)} + \mathrm{THD}_{(L)}{}^2}}{\sqrt{1 + \mathrm{THD}_{(L)}{}^2}} \quad \textbf{(1)}$$

where the value of THD(L) includes the highest compensable harmonic current, defined as double the sampling frequency fs. [7]

The frequency of the highest current harmonic module that can be compensated is the same as one half of the converter switching frequency. The dq-based method operates in a rotary reference frame therefore, the calculated currents must be multiplied by the sin(wt) and cos(wt) signals. By using dq-transformation, the d current component is synchronized with the equivalent phase-to-neutral system voltage, and the q current component is phase-shifted by 90◦.Thesin(wt) and cos(wt) coordinated reference signals are obtained from a synchronous reference frame (SRF) [7] PLL. The SRF-PLL generates a clean sinusoidal waveform even when the scheme voltage is severely indistinct. Tracking errors are eliminated, since SRF-PLLs are considered to evade phase voltage unbalancing, harmonics (i.e., less than 6% and 2% in fifth and seventh, respectively), and counteract caused by the nonlinear load circumstances and measurement errors. Equation shows the affiliation between the real currents iLx(t) (x =a, b, c) and the associated dq elements (id and iq)

$$\begin{bmatrix} i_d \\ i_q \end{bmatrix} = \sqrt{\frac{2}{3}} \begin{bmatrix} \sin\omega t & \cos\omega t \\ -\cos\omega t & \sin\omega t \end{bmatrix} \begin{bmatrix} 1 & -\frac{1}{2} & -\frac{1}{2} \\ 0 & \frac{\sqrt{3}}{2} & -\frac{\sqrt{3}}{2} \end{bmatrix} \begin{bmatrix} i_{Lu} \\ i_{Lv} \\ i_{Lw} \end{bmatrix} \quad \textbf{(2)}$$

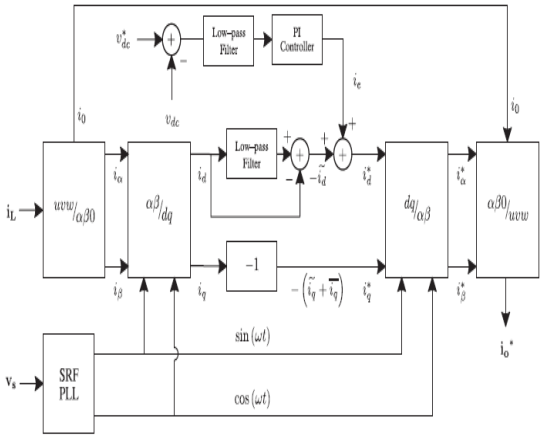

Fig. 4. Current reference generator.

The current reference generator is further connected to the cost function optimization detection algorithm to denote the minimum cost value to generate the pulses. The prediction model produces the i(k+1) [8] value compared to the present value of the measurement. The io(k+1) is given as

$$\mathbf{i_o}[k+1] = \frac{T_s}{L_{\mathrm{eq}}}(v_{xn}[k] - \mathbf{v_o}[k]) + \left(1 - \frac{R_{\mathrm{eq}}\,T_s}{L_{\mathrm{eq}}}\right)\mathbf{i_o}[k] \quad \textbf{(3)}$$

Thus the cost function optimization can be given as

$$g[k+1] = (i^*_{ou}[k+1] - i_{ou}[k+1])^2 + (i^*_{ov}[k+1] - i_{ov}[k+1])^2 + (i^*_{ow}[k+1] - i_{ow}[k+1])^2 + (i^*_{on}[k+1] - i_{on}[k+1])^2 \quad (4)$$

The output current (io) is equivalent to the reference (i∗o) when g =0. Hence, the optimization objective of the cost function is to accomplish a 'g' value close up to zero. The voltage vector vxN that reduces the cost function is selected and then applied at the subsequently sampling state. During the time of each sampling state, the switching state that produces the smallest amount value of 'g' is chosen from the 16 probable function values. The algorithm selects the switching state that generates this negligible value and applies it to the converter throughout the k +1 [8] state.

III. MODELLING OF SMES

In a superconducting coil strong electromagnetic forces caused by the high currents and strong magnetic fields cause big challenges when it comes to the construction of the coil. A large-scale SMES would require rigid supports and a very strong construction. Traditional topologies such as solenoids and toroidal field coils experience these issues strongly. The only current component in the solenoid is in the toroidal direction, see Fig. 5. Axial forces exert compressive stress on the solenoid. Forces in the radial direction, also called hoop forces, cause tensile stress in the toroidal direction which strain to widen the solenoid. In a toroidal field coil (TFC) [9]. The hoop forces which work on each of the solenoids exert tensile stress in the poloidal direction. Compressive stress is generated in the toroidal direction due to the compressive forces which work towards the centre. All these forces require strong constructions in order to not tear the coil apart. SMES has a rather poor energy storage capacity compared to pumped hydro or Compressed Air Energy Storage (CAES). There are conceptual design studies for large scale SMES systems which can operate in diurnal power compensation having the ability to store large amounts of energy. This makes use of several thousand coils to store the energy. However this is only a study case and a real system is not likely to be constructed in the near future.

While the energy density of a SMES [10] system is low, one of the main properties of SMES is the ability to deliver large amounts of energy in a very short time, or said in another way, deliver high power. Combined with very short response time, this makes SMES one of the most suitable energy storage solutions to compensate for fast power fluctuations. Summed up the features of SMES are the following:

- Capability of absorbing and delivering large amounts of power.
- High efficiency.
- Long lifetime.
- Short response time.
- Completely static construction, low maintenance.
- All electric energy storage

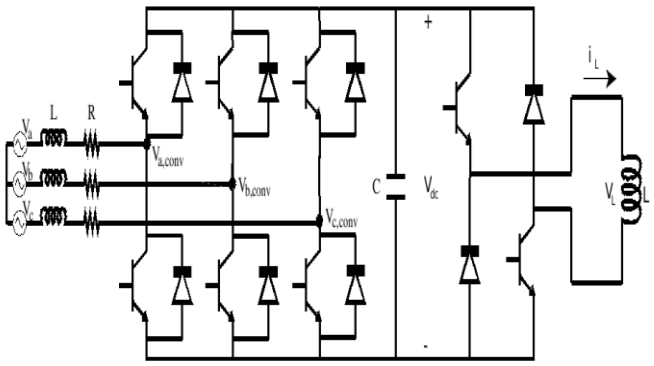

Fig. 5. SMES modeling with STATCOM VSI.

A reverse blocking IGBT would help decreasing these losses as this does not require a blocking diode. On the other hand the VSC/DC-chopper topology has fewer semiconductor devices conducting in the VSC part, but it also has semiconductors in the DC-chopper [10] which contribute to losses. The number of semiconductors the current flows through is actually higher for the VSC/DC-chopper solution than for the CSC. The reason for this is that three half-legs is on compared to two in the CSC. Together with the devices in the chopper this equals five devices to pass compared to four in the CSC. However two of the half-legs in the VSC will share the current making the load on each unit smaller.

IV. SIMULINK RESULTS AND OUTPUTS

Simulation results of this paper is as shown in bellow Figs.6 to 13.

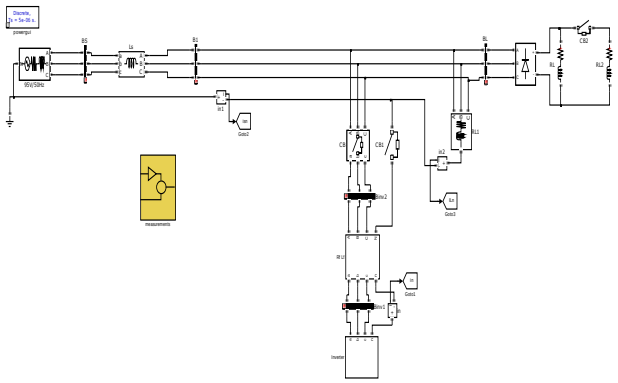

Fig. 6. Test system with Active power filter integrated with SMES.

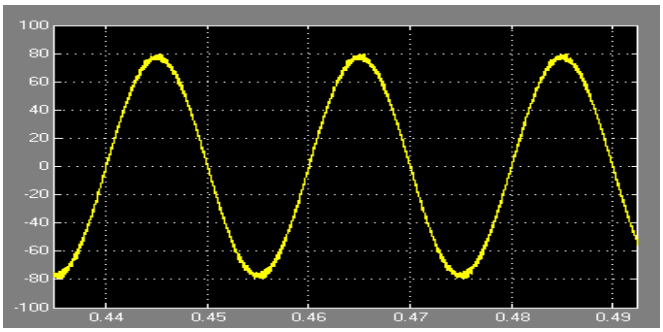

Fig. 7. Source voltage of Phase A.

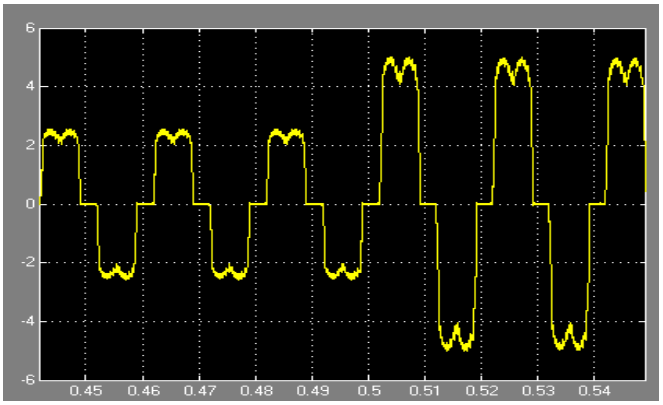

Fig. 8. Load current of Phase A.

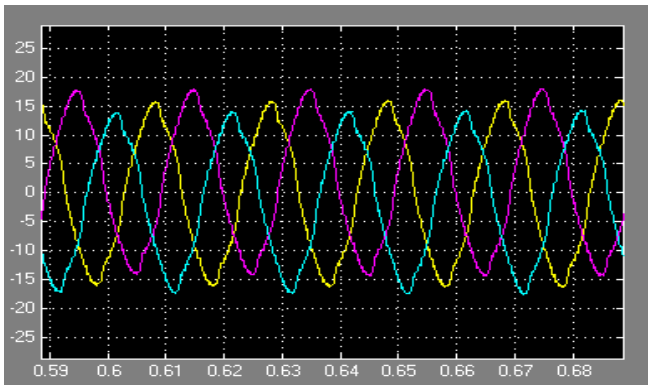

Fig. 9. Source current of three phases.

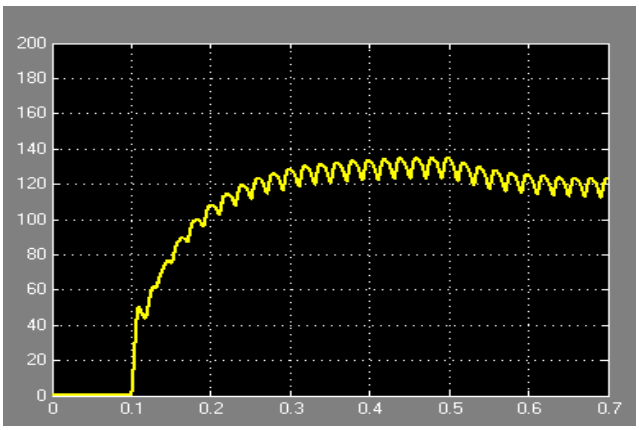

Fig. 10. Vdc (Voltage across capacitor).

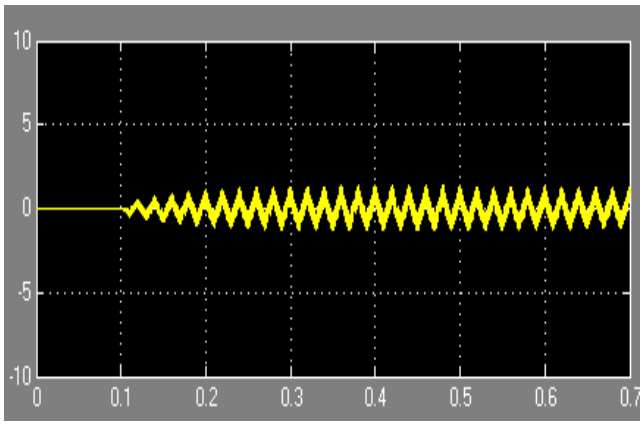

Fig. 11. Neutral current.

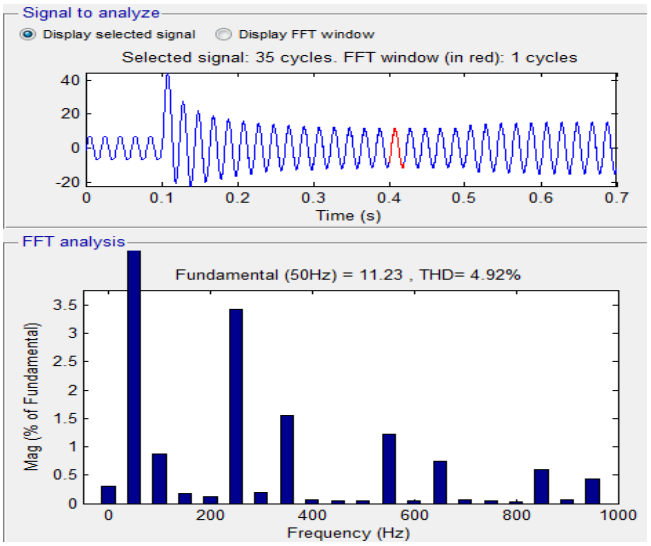

Fig. 12. THD analysis without SMES.

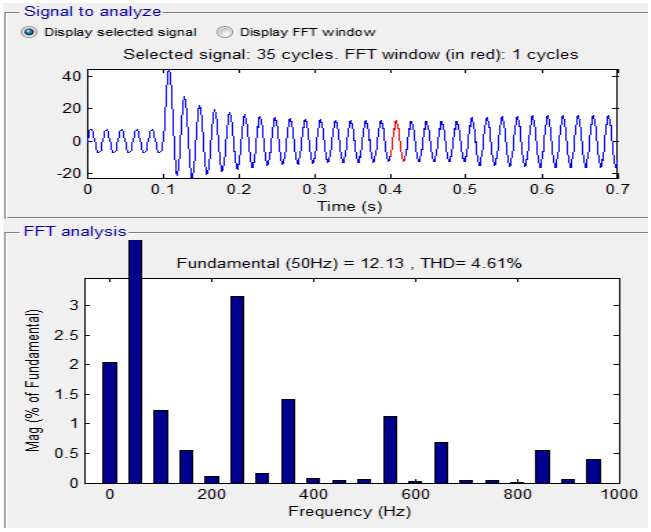

Fig. 13. THD analysis with SMES

V. CONCLUSION

With the above results it can be observed that the source voltage and current and current are improvising after the active power filter is connected to the test system with non linear load. The neutral current of the source is also negligibly low with integration of Active power filter. With an extra attachment of SMES on the DC side of the active power filter the THD of the source current is slightly improved with better enhancement in the amplitude of the current. The results with graphical representation are shown with value calculation and evaluation in section IV.

VI. REFERENCES

[1] F. Wang, J. Duarte, and M. Hendrix, "Grid-interfacing converter systems with enhanced voltage quality for microgrid application;concept and implementation," IEEE Trans. Power Electron., vol. 26, no. 12, pp. 3501– 3513, Dec. 2011.

[2] X. Wei, "Study on digital pi control of current loop in active power filter," in Proc. 2010 Int. Conf. Electr. Control Eng., Jun. 2010, pp. 4287–4290.

[3] R. de Araujo Ribeiro, C. de Azevedo, and R. de Sousa, "A robust adaptive control strategy of active power filters for power-factor correction, harmonic compensation, and balancing of nonlinear loads," IEEE Trans. Power Electron., vol. 27, no. 2, pp. 718–730, Feb. 2012.

[4] J. Rodriguez, J. Pontt, C. Silva, P. Correa, P. Lezana, P. Cortes, andU. Ammann, "Predictive current control of a voltage source inverter," IEEE Trans. Ind. Electron., vol. 54, no. 1, pp. 495–503, Feb. 2007.

[5] P. Cortes, G. Ortiz, J. Yuz, J. Rodriguez, S. Vazquez, and L. Franquelo, "Model predictive control of an inverter with output LC filter for UPS applications," IEEE Trans. Ind. Electron., vol. 56, no. 6, pp. 1875–1883, Jun. 2009.

[6] R. Vargas, P. Cortes, U. Ammann, J. Rodriguez, and J. Pontt, "Predictive control of a three-phase neutral-point-clamped inverter," IEEE Trans. Ind. Electron., vol. 54, no. 5, pp. 2697–2705, Oct. 2007.

[7] P. Cortes, A. Wilson, S. Kouro, J. Rodriguez, and H. Abu-Rub, "Model predictive control of multilevel cascaded H-bridge inverters," IEEE Trans. Ind. Electron., vol. 57, no. 8, pp. 2691–2699, Aug. 2010.

[8] P. Lezana, R. Aguilera, and D. Quevedo, "Model predictive control of an asymmetric flying capacitor converter," IEEE Trans. Ind. Electron., vol. 56, no. 6, pp. 1839–1846, Jun. 2009.

[9] P. Tixador, "Superconducting magnetic energy storage: Status and perspective," IEEE/CSC and ESAS European superconductivity news forum, January 2008.

[10] S. Nomura, N. Tanaka, K. Tsuboi, H. Tsutsui, S. Tsuji-Iio, and R. Shimada, "Design considerations for SMES systems applied to HVDC links," in Power Electronics and Applications, 2009. EPE '09. 13th European Conference on, pp. 1–10, Sept. 2009.

[11] K. F. da Silva and M. Saidel, "Digital control and integration of a 192 mw wind farm with doubly fed induction generator into the brazilian power system," Electric Power Systems Research, vol. 80, no. 1, pp. 108 – 114, 2010.